Available online at www.sciencedirect.com

SciVerse ScienceDirect

Ceramics International 38 (2012) 1687–1696

CERAMICS INTERNATIONAL

www.elsevier.com/locate/ceramint

Dielectric properties of organofunctionalized kaolinite clay and application in adsorption mercury cation

Denis L. Guerra [a,*], Silze P. Oliveira [a], Ricardo A.S. Silva [a], Emiliano M. Silva [a], Adriano C. Batista [b]

[a] University Federal of Mato Grosso, DRM-UFMT, Mato Grosso 78060 900, Brazil
[b] Universidade Estadual do Norte Fluminense, UENF, Rio de Janeiro 28013 02, Brazil

Received 4 June 2011; received in revised form 12 September 2011; accepted 29 September 2011
Available online 6 October 2011

Abstract

Kaolinite clay samples from Amazon region, Pará state, Brazil, were first intercalated with dimethylsulfoxide (DS) followed by immobilization of (3-aminopropyl)triethoxysilane (APS). The samples were characterized by X-ray diffraction, and zero point charge determination. The chemically modified kaolinite samples showed modification of its physical–chemical properties including: specific area of 25.2–421.5 $m^2\ g^{-1}$ for K_1 and $K_{1\text{-DS/APS}}$, and 24.7–425.9 $m^2\ g^{-1}$ for K_2 and $K_{2\text{-DS/APS}}$. New $d_{0\ 0\ 1}$ values of 1.313 and 1.319 nm for the modified kaolinites $K_{1\text{-DS/APS}}$ and $K_{2\text{-DS/APS}}$, respectively, were obtained. From electrical property investigations an increase in electric permittivity was observed for real ($\varepsilon^{|}$) and imaginary ($\varepsilon^{||}$) at low frequencies, which are probably related to the interlayer molecules. The energetic effect caused by mercury cation adsorption was determined through calorimetric titration at the solid–liquid interface and gave net thermal effects that enabled the calculation of the exothermic enthalpic values and the equilibrium constant. From these values negative Gibbs free energy and positive entropy were calculated and this set of thermodynamic data is favorable for mercury/basic center interaction at the solid/liquid interface.

Keywords: C. Dielectric properties; C. Thermal properties; Kaolinite; Adsorption

1. Introduction

Some undesirable heavy metals can be removed from aqueous solutions through chemical precipitation, ion exchange, electrodeposition, solvent extraction, membrane separation, reverse osmosis and adsorption processes [1,2]. For this last procedure, the development of low cost adsorbents with easy manipulation and regeneration for possible reuse has been an object of significant attention, mainly when effluents are involved [1–3]. The clay minerals are abundant in Brazilian soil, especially kaolinite clay, so this clay mineral is easily obtained and can be characterized as a low cost matrix, enabling the development of surface modification processes with high adsorption capacity [4].

Various conventional and non-conventional adsorbents have been explored for removal of different metal ions from aqueous solutions [4–8]. For example, materials containing micro and macropores, such as pillared and intercalated/delaminated clays, are often employed in such operations. In particular, kaolinite and smectite group clay minerals have been successfully explored in many adsorption procedures [4–9]. Organofunctionalization of phyllosilicates can be achieved by either intercalation or grafting of organic molecules on its surface, the surface modification using organophillic cation tetramethylammonium ion to adsorb lead and chromium [10], in our study, the toxic divalent metals Pb^{2+}, Cu^{2+}, Zn^{2+}, and Cd^{2+} were adsorbed onto sulphate and phosphate modified kaolinite clay [11]. Other surface modifications of phyllosilicates were investigated as thermal and acid activations for application in adsorption process [12].

Kaolinite is one of the most important clay minerals and diverse industrial applications depend on the ability to modify the original proprieties for different uses. Many investigations related to dielectric properties and electrical conductivity of minerals, clays and soils have been carried out in recent years [13–15]. The dielectric properties can be changed by means of appropriate structural chemical modifications, for example,

* Corresponding author. Tel.: +55 65 36158951; fax: +55 65 36158951.
E-mail addresses: denis@cpd.ufmt.br, dlguerra@pq.cnpq.br (D.L. Guerra).

0272-8842/$36.00 © 2011 Published by Elsevier Ltd and Techna Group S.r.l.
doi:10.1016/j.ceramint.2011.09.062

through the intercalation process. Dielectrically modified clays are materials with important industrial applications, for instance, in the fabrication of ceramic electric insulators with significant resistance to high voltage electric discharges [13].

The aim of the present investigation is to study the dielectric properties of two different kaolinite types: as originally extracted and when chemically modified. For this purpose the original material was intercalated with dimethylsulfoxide followed by (3-aminopropyl)triethoxysilane immobilization onto the free interlayer kaolinite structure. Those chemical modifications cause not only a considerable increase low frequency permittivity, but also in dielectric properties; this special effect is important for such samples. The end materials were used in aqueous adsorption processes with the mercury cation. The energetic effects caused by mercury cation/basic center interactions on kaolinite at the solid/liquid interface were determined through calorimetric titration procedures.

2. Experimental

2.1. Clay samples

Clay samples used in this investigation were obtained from the Capim River area, Pará State, in the northern part of Brazil. Two distinct samples were obtained in the same geological formation, named K_1 and K_2. The cation-exchange capacities (CEC) were measured to evaluate their potential for intercalation, using the ammonium acetate method with concentrations of 2.0 mol dm^{-3} at pH 8.0. The results gave 0.15 and 0.14 mol g^{-1} for K_1 and K_2 clays, tested after drying in air at room temperature [16,17].

2.2. Separation and purification

The wet sediment clays were soaked in 0.50 dm^3 of distilled water and disaggregated for 24 h by ultrasound. After removal of the sand fraction (>63 μm φ) by sieving, the water was eliminated by centrifuging at 3400 rpm for 1 h. For deflocculation of particles, 1.0×10^{-3} mol dm^{-3} sodium hexametaphosphate were added. Three dispersing agents, 0.15 mol dm^{-3} sodium polyphosphate [16], 5.0×10^{-3} mol dm^{-3} sodium pyrophosphate [18] and 5.0×10^{-3} mol dm^{-3} sodium hexametaphosphate [17] were used to compare their effectiveness for particle separation and influence on the clay minerals. Sodium hexametaphosphate was selected as the most efficient, non-destructive dispersing agent for these clay minerals grains. Silt (2–36 μm φ) and clay (<2 μm φ) fractions were separated by centrifuging three times at 700 rpm using the modified Stoke's law [17].

2.3. Chemical modification

The dimethylsulfoxide was intercalated by direct mixing with an aqueous suspension of natural kaolinite (Scheme 1a). For this process, 5.0 g of kaolinite was mixed in 100.0 cm^3 of dimethylsulfoxide [C_2H_2OS] (Aldrich) in (25.0 cm^3) water at room temperature under vigorous mechanical stirring for 50 h. The resulting suspension was centrifuged at 4000 rpm for 60 min. The liquid portion was decanted to prevent the finest particles from the re-entering suspension, which was dried at 323 ± 1 K for 17 h, to give the $K_{1\text{-DS}}$ and $K_{2\text{-DS}}$ samples (Scheme 1b).

The silane agent used for coupling was (3-aminopropyl)-triethoxysilane [$H_2N–C_3H_6Si(OC_2H_5)_3$] (Aldrich) (Scheme 1c). The first step in this immobilization process consists in suspending, with mechanical stirring, 5.0 g of dried $K_{1\text{-DS}}$ or $K_{2\text{-DS}}$ samples in 100.0 cm^3 of dry toluene. To this suspension 10.0 cm^3 of silylating agent were added and the mixture was stirred for 8 h under an argon atmosphere. The suspension was filtered; the solid was washed with ethanol and water and then dried under vacuum at 320 ± 1 K. The final samples were called $K_{1\text{-DS/APS}}$ and $K_{2\text{-DS/APS}}$, respectively.

2.4. Characterization, adsorption and thermodynamics

Carbon, nitrogen, and hydrogen contents were determined on a Perkin-Elmer 2400 Series II microelemental analyzer. At least two independent determinations were performed for each sample.

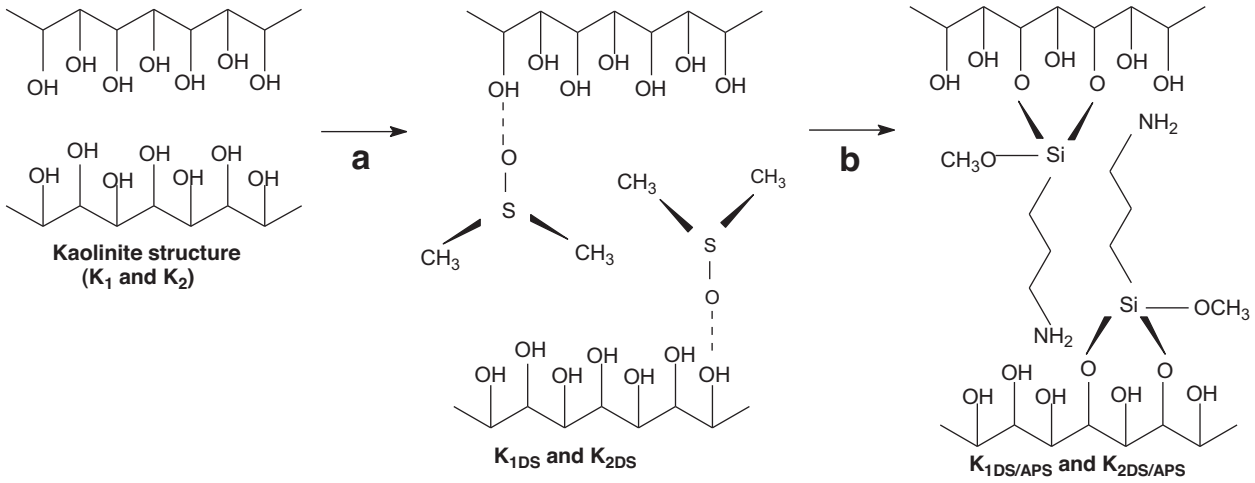

Scheme 1. Schematic representation of intercalation of dimethylsulfoxide (a) followed by immobilization of (3-aminopropyl)triethoxysilane (b).

The natural kaolinite samples were dried at 333 ± 1 K to reach water content in the 12–15% range. X-ray powder diffractometry confirmed the presence of kaolinite clays by conventional sample preparation procedures [19,20]. The preliminary analyses were made with natural samples by several conventional investigations: air-dried, ethyleneglycol solvated and when heated at 573 ± 1 and 773 ± 1 K.

X-ray powder diffraction (XDR) patterns were recorded with a Philips PW 1050 diffractometer using Cu Kα (0.154 nm) radiation between 2° and 65° (2θ) at a speed of 2° per min and steps of 0.050°.

The potentiometric method was used to measure the surface charge density σ_o at different pH. A Systronic pH meter model 362 μ was employed to measure the pH of the solution.

BET (Brunauer–Emmett–Taller) surface areas and porosity measurements of the kaolinite samples were determined using a Quantachome/Nova Surface Area-Pore Volume Analyzer, model 1200/5.01. The micropore size distribution was obtained by applying the BJH (Barret–Joyner–Halenda) method to the adsorption branch of the isotherm.

Dielectric measurements were performed in the frequency 0.10 kHz to 1.00 MHz range measurements by means of an HP 4284A RLC bridge. The capacitor was made of stainless steel and Plexigasss® and consisted of two circular flat electrodes (diameter 13.0 mm) separated by a plastic ring (distance between electrodes 1.5 mm). The powdered sample was filling the space between electrodes. Air capacitance and lead capacitance, necessary for calculation of permittivity, were obtained in a calibration using air and Teflon. Measurements in the frequency range 1.0 MHz to 1.0 GHz were performed by means of an HP 4191A RF impedance analyzer. Before measurements, the equipment was calibrated using standards (air, Teflon). The sample holder (the same as in low-frequency measurements) was mounted on the inner end of a coaxial wave-guide. Measurements in the frequency range 2.5–4.0 GHz were performed with a lumped capacitance method [21,22]. HF generator modulated by 1.0 kHz was used as a source. Standing wave in the slotted line was detected by a microwave diode and nanovoltmeter (Unipan 237). The sample holder and its mounting in a wave-guide were similar as for the frequency range 1.0 MHz to 1.0 GHz.

Samples of about 60.0 mg of unmodified or modified kaolinite were suspended in an aqueous solution containing mercury cation at 298 ± 1 K and pH 3.0 to carry out the adsorption process. The pH was maintained with addition of 0.10 mol dm^{-3} of nitric acid or 0.10 mol dm^{-3} of sodium hydroxide.

Isotherms of concentration versus time were obtained through the batch method [23,24]. The number of moles adsorbed per gram (N_f) was calculated by the difference between the initial (N_i) number of moles of mercury cation and the number of moles of the cation remaining in the supernatant (N_s), divided by the mass (m) of the phyllosilicates used Eq. (1) [25]:

$$N_f = \frac{N_i - N_s}{m} \quad (1)$$

The number of moles of cation adsorbed (N_f) increased with time (t) and as a function of the concentration in the supernatant (C_s), until a plateau related to the saturation of the reactive basic centers located in the kaolinite layered structure. This plateau enables determination of K_L, the Langmuir constant [25–27] given by Eq. (2):

$$\frac{C_s}{N_f} = \frac{1}{K_L b} + \frac{C_s}{b} \quad (2)$$

The shape of isotherm obtained can be used to predict whether an adsorption system [14] in study is ''favorable'' or ''unfavorable'' both in fixed-bed systems, as well as in batch process [28].

The thermal effects from mercury cations interacting on unmodified and modified kaolinite samples were followed in an isothermal LKB 2277 microcalorimetric system. Portions of approximately 10 mg of unmodified or modified kaolinite samples were suspending in 2.0 cm^3 of water in the calorimetric vessel, with vigorous stirring, at 298.15 ± 0.20 K. After calorimetric baseline stabilization, the titrand was incrementally added through a microsyringe coupled to the microcalorimeter, which was connected to a gold needle. For each increment the respective thermal effect was recorded during the progress of the reaction, up to its completion. Mercury nitrate with a concentration of 0.050 mol dm^{-3} was used as cation source and it was added in increments of 10.0 mm^3 [19].

3. Results and discussion

3.1. Elemental analyses

The successful immobilization is clearly expressed by elemental analyses for the natural and chemically immobilized surfaces of kaolinite samples, as listed in Table 1. The samples K_1 and K_2 presented perceptual of hydrogen of 0.22 and 0.26, respectively. These hydrogen atoms existences in the kaolinite structure was attributed of hydroxyl molecules anchored in the interlayer spacing, the perceptual de carbon and nitrogen were not detected in the natural kaolinite samples, this result was indicative of inexistence of organic material in the K_1 and K_2, the organic material can be originated of the depositional and formation medium of kaolinite samples. The degree of organofunctionalization was calculated based on the amount of nitrogen and carbon atoms on the chemically modified kaolinite samples. Based on the analytical data for both nanocompounds, the density of these pendant organic

Table 1
Percentages of carbon (C), hydrogen (H) and nitrogen (N) obtained through elemental analysis for natural kaolinite and for inorganic–organic hybrids and density (d) of the pendant molecules bonded on the silicon layer.

Sample	C (%)	H (%)	N (%)	d (mmol g^{-1})
K_1	–	0.22 ± 0.13	–	–
$K_{1\text{-DS/APS}}$	10.31 ± 0.21	1.42 ± 0.02	5.86 ± 0.02	8.2 ± 0.03
K_2	–	0.26 ± 0.11	–	–
$K_{2\text{-DS/APS}}$	12.22 ± 0.15	2.36 ± 0.01	6.19 ± 0.02	8.8 ± 0.16

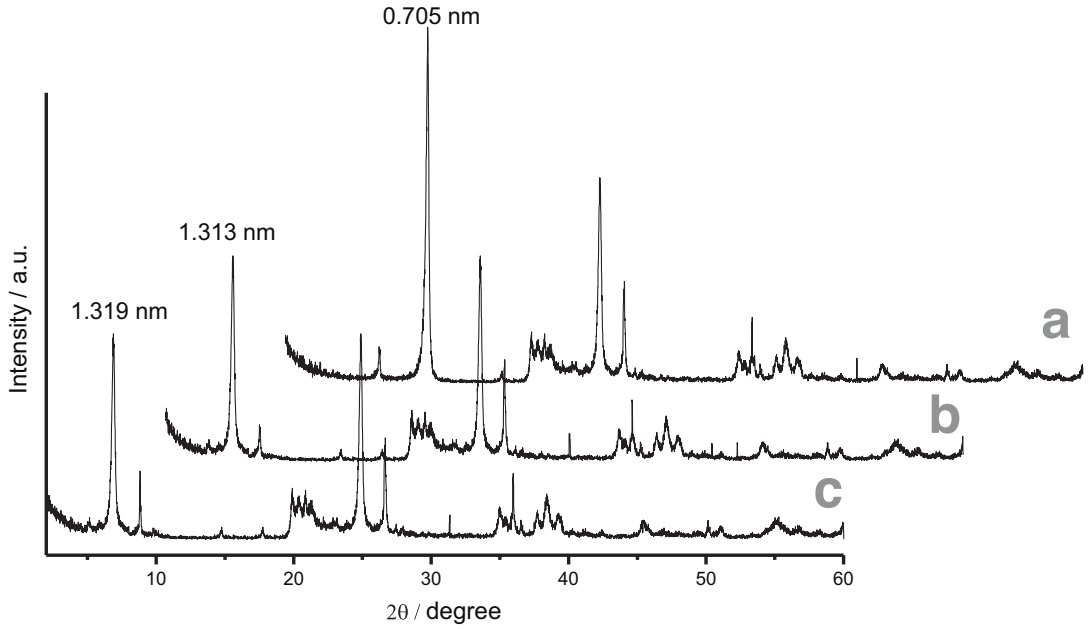

Fig. 1. X-ray diffraction patterns of kaolinite K_1 (a), intercalated and immobilized kaolinites $K_{2\text{-DS/APS}}$ (b) and $K_{1\text{-DS/APS}}$ (c).

molecules immobilized on kaolinite layers can be calculated. Thus, the silylating agents grafted onto kaolinite structure gave an amount of 8.2 ± 0.1 and 8.8 ± 0.2 mmol g^{-1} for $K_{1\text{-DS/APS}}$ and $K_{2\text{-DS/APS}}$ surfaces, respectively.

3.2. X-ray powder diffraction

Total mineralogical composition of the natural clay samples was carried out without oriented mounts and exhibited mainly the presence of kaolinite (principal mineral) and goethite, besides the existence of mica at low concentration (accessory minerals). These considerations are based on preliminary chemical analyses and characteristics X-ray diffraction peaks of natural kaolinite (Fig. 1a). The unmodified and chemically modified kaolinites demonstrated that the basal spacing was increased after the immobilization process. The basal spacing of the natural kaolinite samples changed from 0.705 to 1.312 nm for K_1 and 0.692 to 1.318 nm for K_2. This behavior is attributed to the intercalation, followed by immobilization into the kaolinite structure, as shown in Fig. 1 and represented in Scheme 1. The intensities of the 0 0 1 plane reflection allow calculating the efficiency of the interlayer expansion [18,20]. The mass fraction of the intercalated material can be estimated due to the relative intensities of reflections originating from the unchanged and expanded layers [9]. These samples presented degrees of reaction that could be estimated as 86 and 91% for $K_{1\text{-DS/APS}}$ and $K_{2\text{-DS/APS}}$, respectively.

3.3. Zero charge point

The charge zero points for unmodified and modified kaolinite samples were determined by values of σ_o obtained through potentiometric titration [3], by using Eq. (3):

$$\sigma_o = \frac{F(C_A - C_B + [\mathrm{OH}^-] - [\mathrm{H}^+])}{S_K} \quad (3)$$

where F is the Faraday's constant, C_A and C_B are the concentration of strong acid or base after each addition during titration, $[\mathrm{OH}^-]$ and $[\mathrm{H}^+]$ are the equilibrium concentration of these ions bonded to the surface and S_K is the kaolinite surface area. The plots of σ_o versus pH values for clay samples are shown in Fig. 2.

The intercept point of σ_o with $\mathrm{pH_{zpc}}$ after DS and APS interactions indicated that the surface became more negative. This result aids interaction with species on the surface, being favorable for DS and for APS molecule immobilizations.

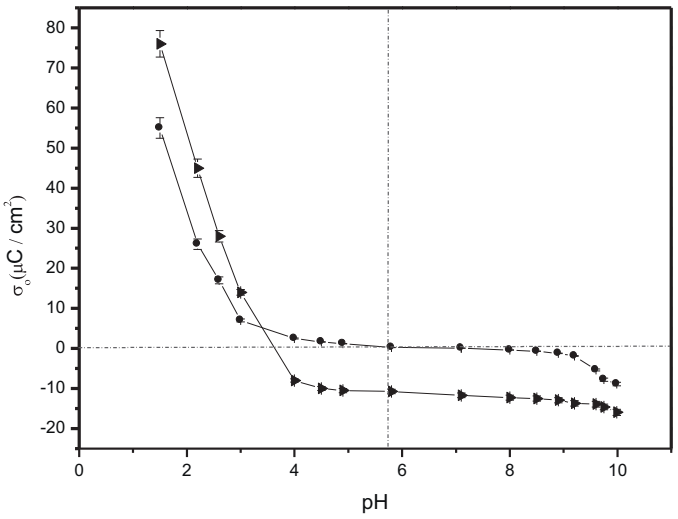

Fig. 2. Potentiometric titration curves depicting the surface charge as a function of pH variation for unmodified kaolinite K_1 (▶) and intercalated and immobilized kaolinite $K_{1\text{-DS/APS}}$ (●).

Table 2
Basal spacing ($d_{0\,0\,1}$), surface area (S), micropore area (M), pore volume (P) and pore diameter (DP) for unmodified (K_1 and K_2) and modified ($K_{1\text{-DS/APS}}$ and $K_{2\text{-DS/APS}}$) kaolinites.

Sample	$d_{0\,0\,1}$ (nm)	S ($m^2\,g^{-1}$)	M ($m^2\,g^{-1}$)	P (nm)	DP (nm)
K_1	0.705	25.2 ± 0.11	8.3 ± 0.13	3.6 ± 0.14	0.23 ± 0.09
$K_{1\text{-DS/APS}}$	1.313	421.5 ± 0.15	110.1 ± 0.15	33.8 ± 0.15	0.81 ± 0.04
K_2	0.692	24.7 ± 0.16	8.4 ± 0.12	3.7 ± 0.04	0.25 ± 0.05
$K_{2\text{-DS/APS}}$	1.319	425.9 ± 0.15	110.1 ± 0.14	33.8 ± 0.11	0.82 ± 0.05

3.4. Textural analysis

The nitrogen adsorption values for kaolinite samples are listed in Table 2. The specific surface areas were calculated by the nitrogen BET method mainly for comparative purposes. The BET surface areas for these kaolinite samples demonstrated that the reaction caused the formation of micro pores in the solid particles, resulting in higher surface areas, giving 25.2 and 421.5 $m^2\,g^{-1}$ ($K_1/K_{1\text{-DS/APS}}$) and 24.7 and 425.9 $m^2\,g^{-1}$ ($K_2/K_{2\text{-DS/APS}}$). The pore volumes were 3.6 and 33.8 nm ($K_1/K_{1\text{-DS/APS}}$) and 3.7 to 33.8 nm ($K_2/K_{2\text{-DS/APS}}$). The pore size distribution in the micropore region was obtained by applying the BJH method from nitrogen isotherms. A change in pore size distribution was observed by comparing unmodified and modified samples. The unmodified samples have mostly micropores in which exhibited the maximum difference in pore volumes, giving 0.23 nm in pore diameter, while for intercalated kaolinite the pore diameter is 0.81 nm. The substantial modification of physicochemical properties of kaolinite samples after organofunctionalization can be attributed to expressive expansion of original kaolinite structure and formation of microcanals in the lamellar phyllosilicate structure. The modified samples presented a unimodal distribution of pore sizes, while unmodified samples showed a bimodal distribution, the existence of micro and macropores can be attributed to these pore size distributions.

3.5. Dielectric measurements

The electric permittivity versus frequency for unmodified K_1 and K_2 kaolinite samples, as well as for DS intercalation and APS immobilization are shown in Fig. 3. The dielectric data obtained at two different calcination temperatures, 373 ± 1 and 673 ± 1 K, for unmodified and modified kaolinite samples at 10.0 kHz, 100.0 MHz and 4.0 GHz are listed in Table 3.

The most important feature is the pronounced increase of permittivity when frequency is lowered and also the strong differences at low frequencies after sample heating. During this process water is removed and the expected differences are obviously related to the adsorbed and/or interlayer water. However, the dielectric properties of chemically modified kaolinite are somewhat different. The permittivity increases very rapidly at low frequencies; therefore, on heating up to 673 ± 1 K, this character does not change considerably. The permittivity for modified kaolinite is higher than those of unmodified kaolinite samples at high frequencies. The main characteristic is the low frequency and the increase seems to disappear when the sample is heated. The observed permittivity dispersion could be explained with the following hypothesis: if molecule relaxation occurs, the time of the hypothetical process should be located at very low frequencies which allow suspecting strongly hindered movement of large molecules or, eventually, some interlayer vibration [13,22].

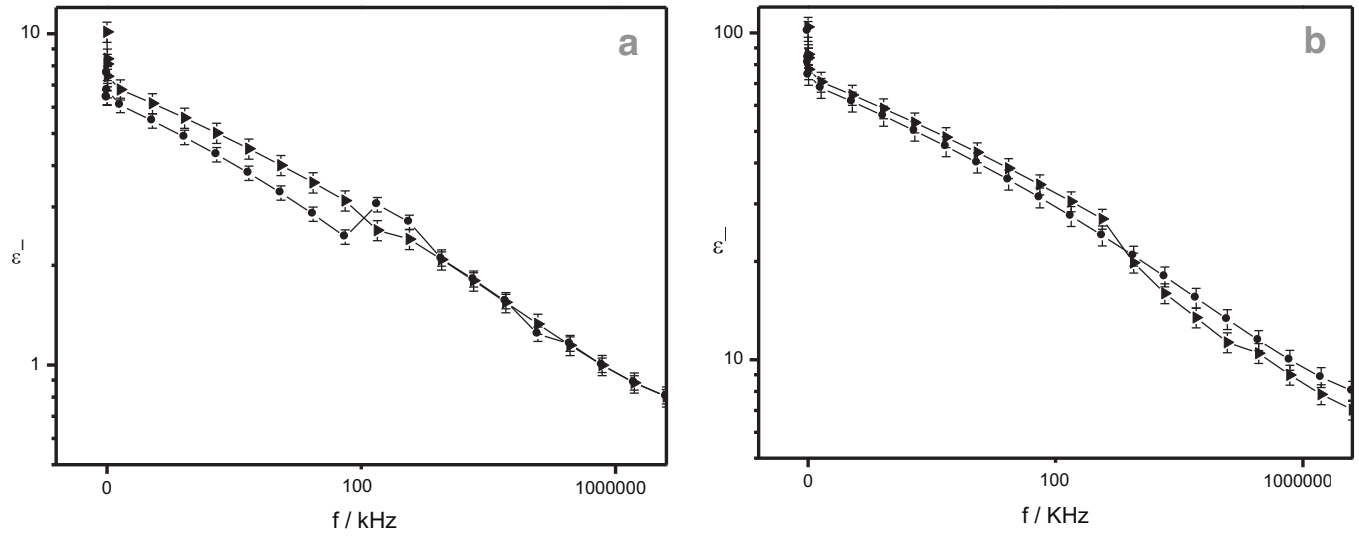

Fig. 3. Real part of the electrical permittivity in K_1 (a) and $K_{1\text{-DS/APS}}$ (b) at 373 (▶) and 673 K (●).

Table 3
Summary of the dielectric properties ($\varepsilon^{|}$, $\varepsilon^{||}$) obtained with unmodified and modified kaolinite samples at 373 ± 1 and 673 ± 1 K.

Sample	$\varepsilon^{|}$ (10 kHz)	$\varepsilon^{||}$ (10 kHz)	$\varepsilon^{|}$ (100 MHz)	$\varepsilon^{||}$ (100 MHz)	$\varepsilon^{|}$ (4 GHz)	$\varepsilon^{||}$ (4 GHz)
K_1	4.38 ± 0.02	0.96 ± 0.05	1.90 ± 0.02	0.03 ± 0.01	1.91 ± 0.05	0.11 ± 0.02
$K_{1–373\ K}$	4.01 ± 0.10	0.78 ± 0.03	1.85 ± 0.11	0.04 ± 0.01	1.81 ± 0.10	0.10 ± 0.01
$K_{1–673\ K}$	1.96 ± 0.02	0.58 ± 0.03	2.00 ± 0.02	0.06 ± 0.01	2.02 ± 0.02	0.01 ± 0.05
$K_{1\text{-DS/ASP}}$	22.7 ± 0.03	68.9 ± 0.02	3.56 ± 0.01	0.40 ± 0.02	2.73 ± 0.01	0.14 ± 0.02
$K_{1\text{-DS/ASP-373 K}}$	19.3 ± 0.01	65.3 ± 0.05	2.99 ± 0.01	0.25 ± 0.01	2.50 ± 0.04	0.22 ± 0.03
$K_{1\text{-DS/ASP-673 K}}$	13.9 ± 0.01	55.0 ± 0.04	2.78 ± 0.02	0.15 ± 0.05	2.31 ± 0.02	0.17 ± 0.01
K_2	3.98 ± 0.02	0.89 ± 0.05	1.87 ± 0.04	0.02 ± 0.09	1.89 ± 0.01	0.10 ± 0.04
$K_{2–373\ K}$	3.05 ± 0.01	0.67 ± 0.01	1.80 ± 0.02	0.03 ± 0.01	1.79 ± 0.01	0.90 ± 0.01
$K_{2–673\ K}$	2.09 ± 0.02	0.49 ± 0.02	1.95 ± 0.06	0.05 ± 0.01	2.03 ± 0.02	0.01 ± 0.02
$K_{2\text{-DS/ASP}}$	21.9 ± 0.03	64.5 ± 0.03	3.18 ± 0.07	0.37 ± 0.01	2.70 ± 0.03	0.12 ± 0.01
$K_{2\text{-DS/ASP-373 K}}$	20.7 ± 0.03	60.4 ± 0.04	3.00 ± 0.04	0.22 ± 0.02	2.35 ± 0.04	0.21 ± 0.06
$K_{2\text{-DS/ASP-673 K}}$	12.7 ± 0.01	52.5 ± 0.03	2.55 ± 0.05	0.13 ± 0.01	2.28 ± 0.02	0.16 ± 0.01

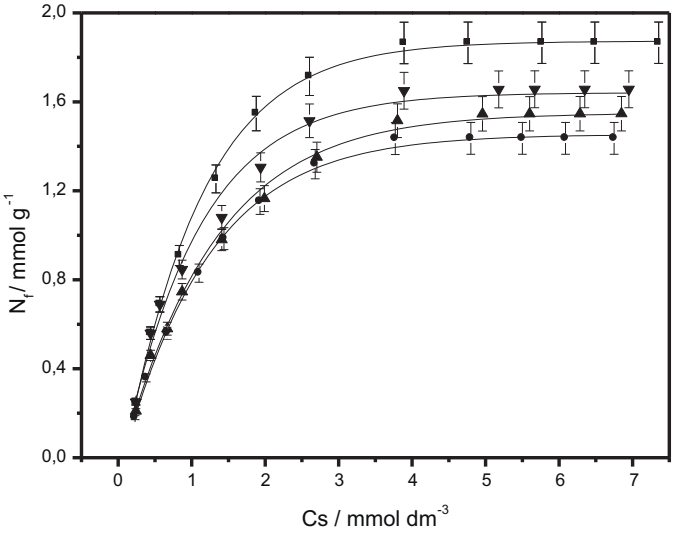

Fig. 4. Mercury adsorption on natural K_1 (▲) and K_2 (●), and chemically modified kaolinites $K_{1\text{-DS/APS}}$ (■) and $K_{2\text{-DS/APS}}$ (▼) at pH 3.0, after 360 min at 298 ± 1 K.

The results obtained for $K_{1\text{-DS/APS}}$ and $K_{2\text{-DS/APS}}$, the real ($\varepsilon^{|}$) and imaginary ($\varepsilon^{||}$) parts of the permittivities are considerably higher in the investigated frequency interval than those observed in the unmodified kaolinite. On heating, the dielectric parameters decrease, but the values are still larger than those in the host materials, in agreement with previous results [13,22].

At very low frequencies 0.1–0.5 kHz resolution was rather poor, ±4.0%, but at the 1.0 kHz to 1.0 MHz frequencies it was much better and estimated as ±0.1%. The resolution at 1.0 MHz to 1.0 GHz frequencies depended on the range. For the frequencies, $10 < f < 800$ MHz, the resolution was approximately 1.0%, whereas in the remaining frequency range it was 10.0% and from 2.6 to 4.0 GHz frequencies the resolution was 5.0% and the absolute errors were considerably larger. With repeated experiments for selected K_1 and K_2 samples the repeatability is close to 20.0%. It has to be mentioned that the dielectric data presented could not be used for absolute parameters due to stress on the investigated materials, since the results depend on the degree of filling the capacitor.

3.6. Adsorption and thermodynamics

The adsorption of mercury cations on unmodified kaolinite and its chemically modified forms are shown in Fig. 4. The influence of the incorporated molecules on kaolinite structure and the alteration of matrix dielectric properties on the adsorption capacity are observed through saturation adsorption values, as represented by the respective isotherms. The results of applying Langmuir adsorption for unmodified kaolinite and its modified forms are listed in Table 4. The Langmuir adsorption model can be used to explain the significant capacities of the chemically modified kaolinite to quantify mercury cation interactions. The Langmuir model presents a significant advantage in comparing the experimental data; it allows quantifying the capacity of retaining cations within the structure of the matrix and to evaluate the constant related to the bonding energy.

The interaction of cations with immobilized external and internal surfaces of the kaolinite structure is governed by the microenvironment around each arrangement, which is usually composed of reactive basic centers, mainly in the internal hydrated structure. Such hydroxyl groups act as bridgings that

Table 4
Adsorption and thermodynamic data for mercury cation adsorption for unmodified and modified kaolinites (pH 3.0, time 360 min at 298.15 ± 0.20 K).

Sample	N_f^{max} (mmol g^{-1})	$K_L \times 10^{-3}$	b	R^2	N_s (mmol g^{-1})	$-\Delta_{int}h$ (J g^{-1})	$-\Delta_{int}H^\circ$ (kJ mol^{-1})	Ln K_L	$-\Delta_{int}G^\circ$ (kJ mol^{-1})	$\Delta_{int}S^\circ$ (J K^{-1} mol^{-1})
K_1	1.55 ± 0.12	8.83 ± 0.13	1.78	0.999	1.54 ± 0.12	11.15 ± 0.13	7.24 ± 0.11	9.09	22.5 ± 0.1	51 ± 1
$K_{1\text{-DS/ASP}}$	1.87 ± 0.11	11.05 ± 0.12	2.05	0.998	1.76 ± 0.13	12.36 ± 0.14	7.02 ± 0.12	9.31	23.1 ± 0.2	54 ± 1
K_2	1.43 ± 0.12	9.71 ± 0.11	1.65	0.997	1.61 ± 0.13	11.62 ± 0.15	7.22 ± 0.12	9.18	22.8 ± 0.2	52 ± 1
$K_{2\text{-DS/ASP}}$	1.65 ± 0.11	12.17 ± 0.15	1.98	0.999	1.91 ± 0.11	12.57 ± 0.17	6.58 ± 0.11	9.41	23.3 ± 0.1	56 ± 1

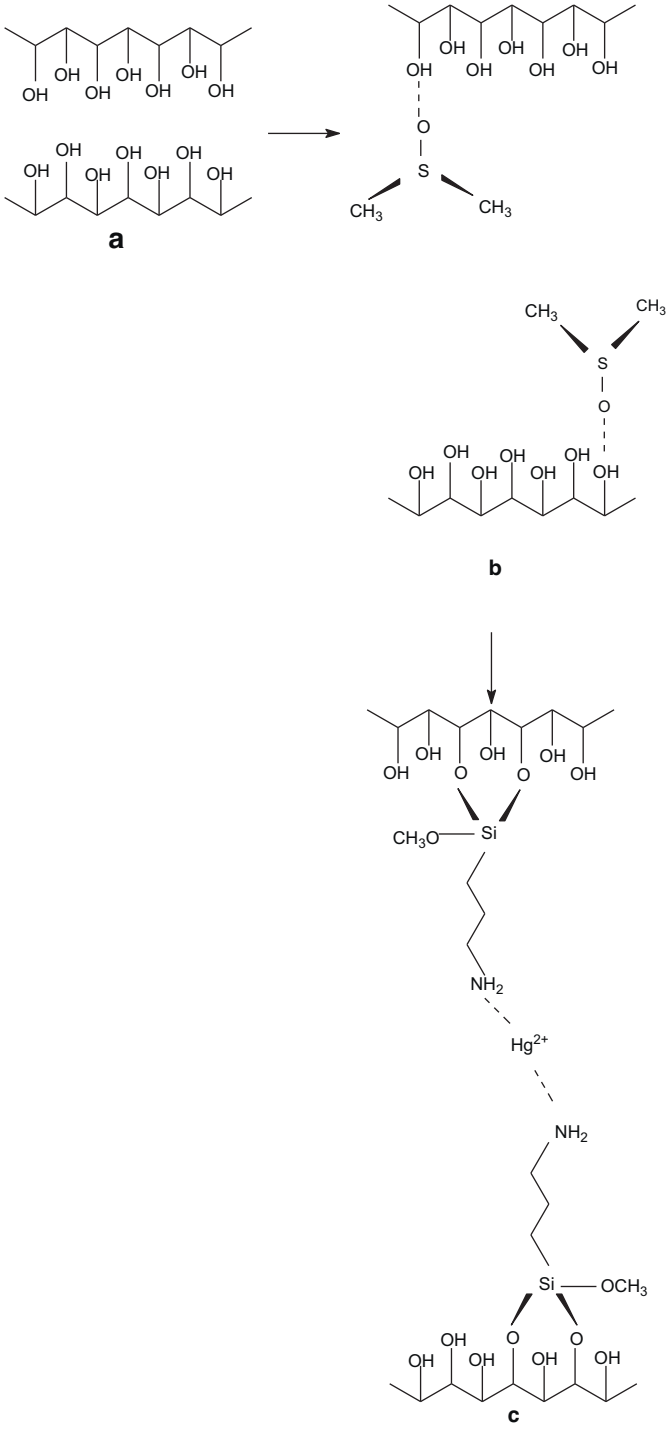

Scheme 2. Schematic representation of intercalation followed by immobilization: interlayer spacing (a), dimethylsulfoxide intercalation (b) and immobilization with complexed mercury (c).

favor the kaolinite matrix intercalation process. The schematic representation of DS intercalation, followed by APS immobilization and the proposed reactive centers for adsorption are shown in Scheme 2. As the dimethylsulfoxide molecule was used in a first step for interlayer expansion (Scheme 2b) of the structure in the original kaolinite (Scheme 2a), the entrance of APS molecules is made easier by the entrance of DS molecules (Scheme 2c). This process gives the pendant anchored chains with available amino groups inside the interlayer space, available to bond to appropriate cations, such as mercury.

The adsorption process was evaluated from the results obtained, by considering the adsorption isotherms and the molar fraction of the mercury cation in solution. The data were adjusted to a Langmuir model, in which it assumed that monolayer of mercury cations is formed on the chemically modified kaolinite surface. For this model the results obtained were adjusted to Eq. (2). The maximum adsorption capacities, N_f^{max}, for mercury onto unmodified and modified kaolinite are listed in Table 4, which values are highest for chemically modified kaolinites. This behavior is attributed to the optimization of the physical chemical and dielectric properties and, consequently, to the larger surface capacity to bond species.

The influence of electrical permittivity variation on the mercury adsorption process can be observed in Fig. 5. The alteration in electric charges onto internal surfaces of the kaolinite structure can be interfered in the adsorption capacity of modified kaolinite, which feature is observed through the variations due to calcination temperatures of 373 ± 1 and 673 ± 1 K. The ionic and electrical transports on the surface are directly influenced by elimination of hydrating water in the kaolinite structure while the available silanol and amino groups in this structure promote the new electronic contribution on the internal surfaces. From the macroscopically inhomogeneous kaolinite it is possible to observe the Maxwell–Wagner effect [13,22], arising from accumulation of charge or hydroxyl groups in intergranular areas and, therefore, formation of macro-dipoles and permittivity dispersion, which effect that can be maximized by introduction of interlayer molecules in the structure. The dispersion could also be the result of a collective movement of the interlayer hydrating water molecules and formation of macroscopic polarization, this effect is formally similar to Maxwell–Wagner dispersion [13,21,22].

From the adsorption isotherm for mercury cation, represented by a C_s versus N_f plot, the angular coefficient can be obtained and its linearized form, C_s/N_f versus C_s, provides the linear coefficient, as shown in Fig. 4, whose data were adjusted to the Langmuir model, as before. For a series of calorimetric titrations, the number of increments and the volumes of mercury cation needed to saturate the mass of the kaolinite [28] are listed in Table 4.

The molar fraction of the mercury cation in the supernatant in equilibrium for each point of the calorimetric titration (X) was calculated by considering the number of moles of the solute (N_s) and the number of moles of water (N_{wat}) [28,29].

$$X = \frac{N_s}{N_s + N_{wat}} \tag{4}$$

The calculated X values and the data obtained from calorimetry were adjusted to the modified Langmuir model [29,30] expressed by Eq. (5). The calorimetric results are presented in Figs. 6 and 7 and are listed in Table 4.

$$\frac{\sum X}{\sum \Delta h_r} = \frac{1}{(K-1)\Delta_{\text{int}} h} + \frac{\sum X}{\Delta_{\text{int}} h} \tag{5}$$

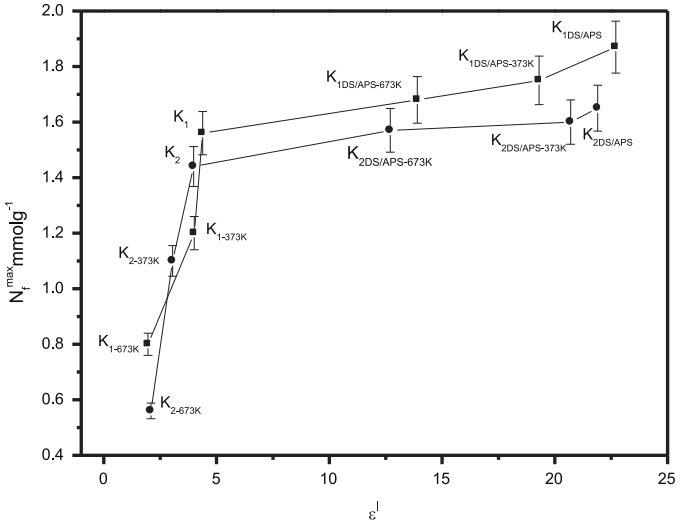

Fig. 5. Maximum adsorption capacity at equilibrium, N_f^{max} as a function of electrical permittivity for natural K_1 (■) and K_2 (●), and for calcinated chemically modified kaolinites at 373 and 673 K at pH 3.0, after 360 min at 298 ± 1 K.

where $\Sigma\Delta h_r$ is the thermal effect of mercury-modified kaolinite surface interaction, Δh_{int} is the thermal effect of formation of the mercury monolayer on the modified kaolinite surface, and K is a proportionality constant that also includes the equilibrium constant.

The isotherm data obtained from the calorimetric titrations were used in a $\Sigma\Delta h_r$ versus ΣX plot and the linearized form is given by a $\Sigma X/\Sigma\Delta h_r$ versus ΣX plot [28,29]. One example of linearization involving mercury cation adsorption is shown in Fig. 7, from which the angular and linear coefficients could also be obtained. After adjusting the data to the modified Langmuir equation, the resulting values were applied to find $\Delta_{int}h$ values that are the thermal effect of the monolayer. From these data the values of constant K_L can be calculated.

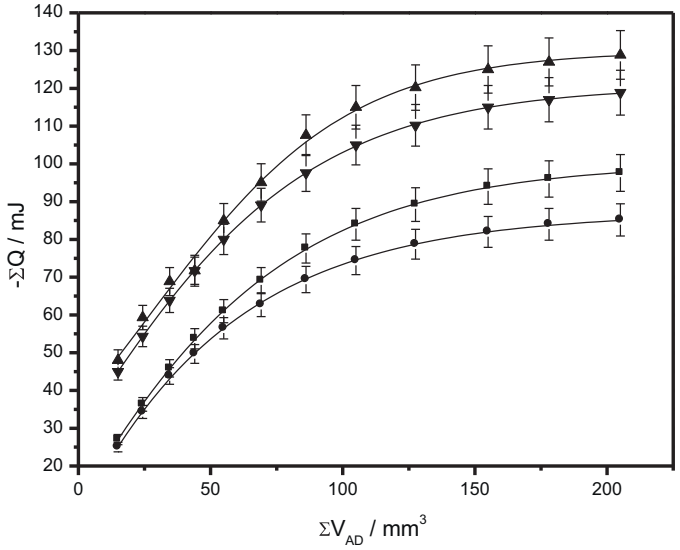

Fig. 6. Isotherms of thermal effects for mercury adsorption for K_1 (▲) and K_2 (●) and for chemically modified kaolinites $K_{1\text{-DS/APS}}$ (■) and $K_{2\text{-DS/APS}}$ (▼) at pH 3.0, after 360 min at 298 ± 1 K.

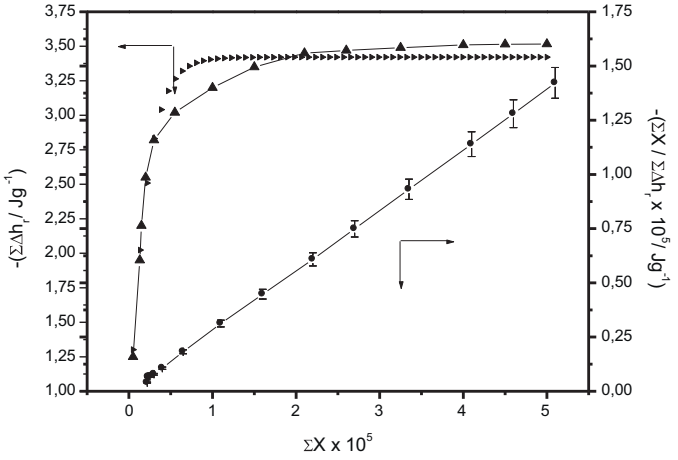

Fig. 7. Isotherm for calorimetric titration of about 10 mg of chemically modified kaolinites $K_{1\text{-DS/APS}}$ and $K_{2\text{-DS/APS}}$ suspended in 2.0 cm^3 of 5.0 × 10^{-2} mol dm^{-3} at 298.15 ± 0.20 K. The straight line is the isotherm in linearized form.

From the enthalpy of formation of monolayer Δh_{int} and the number of moles of mercury, N_s, adsorbed, on the modified kaolinite matrix, the enthalpies of interaction can be calculated by Eqs. (6) and (7) [28]:

$$\Delta_{int}H = \frac{\Delta_{int}h}{N_s} \tag{6}$$

$$\frac{1}{\Delta_{int}h} = \beta \tag{7}$$

where β is the angular coefficient obtained from Eq. (7). Taking these values into account:

$$\Delta_{int}G = -RT\ln K_L \tag{8}$$

where K_L is the equilibrium constant obtained from the Langmuir model, T is the absolute temperature, the universal gas constant $R = 8.314 \times 10^{-3}$ kJ K^{-1} mol^{-1}. Eq. (9) relates the energies involved.

$$\Delta_{int}G = \Delta_{int}H - T\Delta_{int}S \tag{9}$$

The thermodynamic cycle for this series of adsorptions involving a suspension (susp) of natural and modified kaolinite samples (K_X) in aqueous (aq) solution with mercury cation (M^{2+}) can be represented by the following calorimetric reactions. Reactions (10)–(12) represent calorimetric titration experiment carried out in duplicate for each determination:

$$K_{X(susp)} + M^{2+}{}_{(aq)} \rightarrow K_X{\cdot}M^{2+}{}_{(susp)} \qquad \Sigma Q_t \tag{10}$$

$$K_{X(susp)} + nH_2O \rightarrow K_X{\cdot}nH_2O_{(aq)} \qquad \Sigma Q_h \tag{11}$$

$$M^{2+}{}_{(aq)} + nH_2O \rightarrow M^{2+}{\cdot}nH_2O_{(aq)} \qquad \Sigma Q_d \tag{12}$$

The thermal effects of reactions (10)–(12) for each experimental point of the calorimetric titration were considered in the calculation of the net thermal effect (ΣQ_r) of these interactions, as represented by reaction (13).

$$K_X{\cdot}nH_2O_{(aq)} + M^{2+}{\cdot}nH_2O_{(aq)} \rightarrow K_X{\cdot}M^{2+}{}_{(susp)} + 2nH_2O \qquad \Sigma Q_r \tag{13}$$

As the thermal effect of the kaolinite hydration is null, then the net thermal effect for the complete calorimetric titration is given by $\Sigma Q_r = \Sigma Q_t - \Sigma Q_d - \Sigma Q_h$ [27], as represented by Eq. (13), and shown by the experimental data of the isotherms in Fig. 7. From the equilibrium constant the Gibbs free energy was calculated from Eq. (8) and combined with the enthalpic value, the entropy can also be calculated by Eq. (9).

A summary of the thermodynamic values obtained in the present study involving mercury cation with modified kaolinite samples is given in Table 4, showing exothermic enthalpic effects results from the chemical modification process. In all cases, the Gibbs free energy for the chemically modified kaolinite samples demonstrated that the interaction of mercury cation with the modified kaolinite samples occurred in a spontaneous way. The entropic values were practically constant, suggesting that a similar behavior occurred in the system, during bond formation. The missing thermodynamic data, the entropy values are also listed in Table 4. These values suggest that, during complex formation, the desolvation disturbs the structure of the reaction medium to promote the disorganization of the system and, consequently, leads to an increase in entropy [28,29]. The highest entropic values have been observed for cations with the largest hydration volumes and illustrate the principle that the loss of water of hydration leads to a disorganization of the final systems [28,29]. In conclusion, all thermodynamic values are favorable, with exothermic enthalpy, negative free Gibbs energy and positive entropy, data corroborate with mercury cation/$K_{1\text{-DS/APS}}$ and $K_{2\text{-DS/APS}}$ interaction at the solid/liquid interface.

4. Conclusions

Kaolinite from the Amazon region presented compatibility with dimethylsulfoxide intercalation, followed by (3-aminopropyl)triethoxysilane immobilization. Following this chemical modification process, the physical–chemical and dielectric properties were altered, the chelating materials can be to use for heavy metals recovery from aqueous waste or systems on large scale. The degree of reaction is estimated as above 85% for modified kaolinite, an efficiency that was shown by the increased percentage of substituent groups. Analyzing the dielectric behavior after DS/APS reactions was investigated, indicative that the low frequency permittivity was considerably higher for the modified kaolinite than that observed for unmodified kaolinite. The common feature was also the decrease of permittivity $\varepsilon^{|}$, the same was observed for $\varepsilon^{||}$, when the material was heated. The low frequency properties could be, partly at least, related to the content of water. It is seems the change of dielectric properties is related to the collective movements of the incorporated molecules inside the free cavity of these natural and modified kaolinite samples. However, convenient selection of these molecules can increase dielectric permittivity and losses over a much larger frequency interval.

The adsorption capacity of modified kaolinite was promoted by the new electric and physical–chemical properties. The electronic density in chemically modified kaolinite surfaces can be altered by amino groups introduced through immobilization agents and by hydrating water molecules as the process progresses. The increasing reactivity of the electronic center on kaolinite sample surfaces can be interfered in the mercury adsorption process. The quantitative mercury cation/reactive basic center interactions on the chemically modified clay followed by calorimetric titration demonstrated that the interaction at the solid/liquid interface gave favorable sets of thermodynamic data, such as exothermic enthalpy, negative Gibbs free energy and positive entropic values.

Acknowledgements

The authors are indebted to CNPq for fellowships and CAPES for financial support.

References

[1] K.G. Bhattacharyya, S.S. Gupta, Pb(II) uptake by kaolinite and montmorillonite in aqueous medium: influence of activation of the clays, Colloids Surf. A 277 (2006) 191–200.
[2] H. Koyuncu, A.R. Kul, N. Yildiz, A. Çalimli, H. Ceylan, Equilibrium and kinetic studies for the sorption of 3-methoxybenzaldehyde on activated kaolinites, J. Hazard Mater. 40 (2007) 489–497.
[3] D.M. Manohar, B.F. Noeline, T.S. Anirudhan, Adsorption performance Al-pillared betonite clay for the removal of cobalt (II) from aqueous phase, Appl. Clay Sci. 31 (2006) 194–206.
[4] D.L. Guerra, C. Airoldi, The performance of urea-intercalated and delaminated kaolinite-adsorption kinetics involving copper and lead, J. Braz. Chem. Soc. 20 (2009) 19–30.
[5] N. Temkin, E. Kadinci, Ö. Demirbas, M. Alkan, A. Kara, Adsorption of polyvinylimidazole onto kaolinite, J. Colloid Interface Sci. 89 (2006) 472–479.
[6] N. Wada, R. Raythatha, S. Minomura, Pressure effects on water-intercalated kaolinite, Solid State Commun. 63 (1987) 783–786.
[7] H.H. Tran, F.A. Roddick, J.A. O'Donell, Comparison of chromatography and desiccant silica gel for the adsorption of metal ions. I. Adsorption and kinetics, Water Res. 7 (2003) 471–478.
[8] B. Yu, Y. Zang, A. Shukla, S.S. Shukla, K.L. Dorris, The removal of heavy metals from aqueous solution by sawdust adsorption-removal of copper, J. Hazard. Mater. B 80 (2000) 33–42.
[9] J.J. Tunney, C. Detellier, Intercalation of alkylamines and water into kaolinite with methanol kaolinite as an intermediate, Chem. Mater. 8 (1996) 927–932.
[10] F. Cadena, R. Rizvi, R.W. Peters, Feasibility studies for the removal of heavy metals from solution using tailored bentonite, in: Proceedings of the 22nd Mid Atlantic Industrial Waste Conference on Hazardous and Industrial Wastes, Drexel University, 1990.
[11] K.O. Adebowale, I.E. Unuabonah, B.I. Olu-Owolabi, Adsorption of some heavy metal ions on sulfate- and phosphate-modified kaolin, Appl. Clay Sci. 29 (2005) 145–148.
[12] E.G. Pradas, M.V. Sanchez, F.C. Cruz, M.S. Viciana, M.F. Perez, Adsorption of cadmium and zinc from aqueous solution on natural and activated bentonite, J. Chem. Technol. Biotechnol 59 (1994) 289–295.
[13] K. Orzechowski, T. Slonka, J. Glowinski, Dielectric properties of intercalated kaolinite, J. Phys. Chem. Solids 67 (2006) 915–922.
[14] H. Zıpkın, L. Israel, S. Güler, Ç. Güler, Dielectric properties of sodium fluoride added kaolinite at different firing temperatures, Ceram. Int. 33 (2007) 663–667.
[15] Y. Pu, K. Chen, H. Wu, Effects of kaolinite addition on the densification and dielectric properties of $BaTiO_3$ ceramics, J. Alloys Compd. 509 (2011) 8561–8566.
[16] R. Petschick, G. Kuhn, F. Gingele, Clay minerals distribution surface sediments of the south Atlantic: sources, transport and relation to oceanography, Mar. Geol. 130 (1996) 203–229.
[17] H. Shizozu, Introduction to clay mineralogy-fundamentals for clay science, Asakura Pub. Jpn. 1 (1988) 68–79.

[18] D.M. Moore, R.C. Reynolds Jr., X-ray Diffraction and the Identification and Analysis of Clay Minerals, 2nd ed., Oxford University Press, Oxford, 1997.
[19] D.L. Guerra, C. Airoldi, R.R. Viana, Performance of modified montmorillonite clay in mercury adsorption process and thermodynamic studies, Inorg. Chem. Commun. 11 (2008) 20–24.
[20] D.L. Guerra, V.P. Lemos, C. Airoldi, R.S. Angélica, Influence of the acid activation of pillared smectites from Amazon (Brazil) in adsorption process with butylamine, Polyhedron 25 (2006) 2880–2890.
[21] H.A. Kołodziej, M. Pajdowska, L. Sobczyk, Lumped-capacitance method applied to measurements of complex dielectric permittivity in polar liquids from 100 to 3 GHz, J. Phys. E Sci. Instrum. 11 (1978) 752–762.
[22] N.E. Hill, V.E. Vaughan, A.H. Prince, M. Davies, Dielectric properties and molecular behaviour, in: T.M Sugden (Ed.), The van Norstrand Series in Physical Chemistry, New York, Toronto, Melbourne, 1969, p. 282.
[23] M.G. Fonseca, C. Airoldi, Action of silylating agents on a chrysotile surface and subsequent reactions with 2-pyridine and 2-thiophene carbaldehydes, J. Chem. Soc. Dalton Trans. 42 (1999) 3687–3692.
[24] R.S.A. Machado, M.G. Fonseca, L.N.H. Arakaki, S.F. Oliveira, Silica gel containing sulfur, nitrogen and oxygen as adsorbent centers on surface for removing copper from aqueous/ethanolic solutions, Talanta 63 (2004) 317–322.
[25] M.O. Machado, A.M. Lazarin, C. Airoldi, Thermodynamic features associated with intercalation of some n-alkylmonoamines into barium phosphate, J. Chem. Thermodyn. 38 (2006) 130–136.
[26] V.S.O. Ruiz, C. Airoldi, Thermochemical data for n-alkylmonoamine intercalation into crystalline lamellar zirconium phenylphosphonate, Thermochim. Acta 420 (2004) 73–78.
[27] O.A.C. Monteiro, C. Airoldi, The influence of chitosans with defined degrees of acetylation on the thermodynamic data for copper coordination, J. Colloid Interface Sci. 282 (2005) 32–37.
[28] A.M. Lazarin, C. Airoldi, Thermochemistry of intercalation of n-alkylmonoamines into lamellar hydrated barium phenylarsonate, Thermochim. Acta 454 (2007) 43–49.
[29] P.D. Padilha, J.C. Rocha, J.C. Moreira, J.T.D. Campos, C.D. Federici, Preconcentration of heavy metal ions from aqueous solutions by means of cellulose phosphate: an application in water analysis, Talanta 45 (1997) 317–323.
[30] A.I. Martin, M. Sanchez-Chaves, F. Arranz, Synthesis, characterization and controlled release behaviour of adducts from chloroacetylated cellulose and α-naphthylacetic acid, React. Funct. Polym. 39 (1999) 179–187.